Cazorla-Marín, A.; Montagud- Montalvá, C.; Tinti, F.; Corberán, JM. (2019). A novel TRNSYS type of a coaxial borehole heat exchanger for both short and mid term simulations: B2G model. Applied Thermal Engineering. 164(114500):1-15. https://doi.org/10.1016/j.applthermaleng.2019.114500

A novel TRNSYS type of a coaxial borehole heat exchanger for both short and mid term simulations: B2G model

Antonio Cazorla-Marín[a]*, Carla Montagud-Montalvá[a], Francesco Tinti[b], José Miguel Corberán[a]

[a] Instituto Universitario de Investigación de Ingeniería Energética (IUIIE), Universitat Politècnica de València, 46022 València, Spain

[b] Department of Civil, Chemical, Environmental and Materials Engineering, University of Bologna, via Terracini 28, 40131 Bologna, Italy. E-mail: francesco.tinti@unibo.it

*Corresponding author: ancamar4@upvnet.upv.es

Abstract

A dynamic model of a ground source heat pump system is a very useful tool in order to optimize its design and operation. In order to fairly predict the performance of such a system, the dynamic evolution of the fluid entering the heat pump and coming from the borehole heat exchanger (BHE) must be accurately reproduced not only in the long term but also in the short-mid term operating conditions, as it directly affects the coefficient of performance of the heat pump unit.

In this context, the B2G model was developed to reproduce the short-term dynamic evolution of the fluid temperature inside the BHE. This work presents the new upgraded version of the B2G dynamic model for a coaxial BHE, which includes several new features to better reproduce not only the short-term but also the mid-term behaviour of the BHE. For that purpose, the model of the surrounding ground has been improved: vertical heat conduction in the grout and ground, heterogenous ground with different layers, and a higher number of ground nodes in the thermal network considered in the model were added, which are automatically located by means of polynomial correlations for any type of ground, geometry and operating conditions. This novel approach has been implemented in TRNSYS for accurately modelling the dynamic behaviour of a coaxial BHE with low computational cost.

The model has been validated against experimental data from a dual source heat pump installation in Tribano (Padua, Italy) and has proven capable of accurately reproducing the short-mid term (up to five days) behaviour of the BHE.

Keywords

Ground Source Heat Pump; Borehole Heat Exchanger; Dynamic modelling; B2G model; Coaxial Borehole Heat Exchanger.

1 Introduction

The global warming, oil dependency and carbon emissions are important environmental problems to address, leading to a growing research in alternative and renewable energy sources, as well as the improvement of the energy effiency of the systems. In the building sector, heating and cooling systems represent an important and growing part of the total energy consumption [1]. In this context, Ground Source Heat Pump (GSHP) systems represent an efficient alternative to conventional systems [2,3]. They contribute to energy savings in comparison with air-to-water heat pumps [4], since the ground temperature is more constant than that of the air during the year and, in most cases, it is more favorable than the air as a source.

This advantage should not be spoiled with a low efficiency of the system components and their operation. Thus, it is important to optimize them in order to achieve the highest possible efficiency of the entire system. Among all the components of a GSHP systems, the Ground Source Heat Exchanger (GSHE) is one of the most important and relatively expensive, as it implies the drilling in the ground and the installation of long pipes in order to extract/inject heat from/to the ground. For this reason, the correct design of this GSHE field, as well as the optimization of the whole system is of outmost importance in order to compete with other conventional technologies. Hence, the design of this heat exchanger must be optimized in order to obtain a good efficiency, at a reasonable cost, in the heat transfer process with the ground. In practice, this trade-off between efficiency and cost means that the GSHE should not be under-sized (low efficiency) or over-sized (high cost).

Inside the GSHE market, there exist different configurations [5], but the most common is the vertical heat exchanger, also known as Borehole Heat Exchanger (BHE). In this configuration, a vertical heat exchanger is drilled into the soil. Among the common types of BHEs, the most widespread is the single U-pipe, but it is not the most efficient from a heat transfer point of view. Other configurations of BHEs have been studied in order to obtain a low thermal resistance and thus, improve the heat transfer efficiency between the fluid and the ground. One of the configurations that have presented an increase in the current research and development activities is the coaxial BHE [6]. For example, Kurevija et al. [7] studied the suitability of coaxial BHEs for active and passive cooling, determining that they need to be designed with active cooling option; Acuña [8] studied different configurations (U-pipes, coaxial, multi-pipe and multi-chamber BHEs) in order to reduce the temperature difference between the fluid and the surrounding ground, carrying out several experimental tests with these configurations. Other improvements have also been studied, like the immersion of the vertical probes in an artificial fluid inside a case, increasing the heat transfer within the borehole due to natural convection [9].

Regarding the design and optimization of the GSHP systems, dynamic models are a very useful tool, as they are able to predict the behaviour of the whole integrated system. Focusing on the most important component in GSHP systems, the BHE, an accurate short-term dynamic model is necessary, especially in an ON/OFF operation GSHP system, where it is key to reproduce accurately the cycling of the system, because its performance will strongly depend on the return temperature coming from the ground loop. Against this background, there exist several BHE models with different level of complexity, starting from the common analytical models, focused on the prediction of the ground temperature variation: Infinite Line Source (ILS), Infinite Cylindrical Source (ICS) or Finite Line Source (FLS), based on the work of Carslaw and Jaeger [10]. With these models it is possible to calculate the ground temperature outside the BHE, simulating the heat conduction in a homogeneous soil mass with a constant heat flow rate from a BHE, under different assumptions and levels of complexity. These models have been used as the base to develop a great part of the current analytical

and semi-analytical models [11]. On the other hand, several numerical and analytical models with a higher level of detail have been developed, modelling not only the surrounding ground, but also the behaviour of the borehole in terms of the fluid temperature evolution. Numerical models, most of them based on the finite difference and the finite element (FEM) methods[11], are usually more precise and flexible than analytical models, but they have a higher computational cost and it is more difficult to couple them with dynamic simulation programs. On the other hand, analyitical and semi-analyitical methods are limited to some assumptions and simplifications that reduce their accuracy. However, they present a lower computational cost and they can be coupled into design/simulation programs more easily [12]. Several of these models use a thermal network based on thermal resistances and capacitances in order to model the heat transfer between the borehole and the surrounding ground [13–17]. Among them, Zarrella et al. [18] presented the CaRM (Capacity and Resistance) model, considering the thermal capacitance of the borehole: grout and fluid. Also the TRCM (Thermal Resistance Capacity Model) developed by Bauer et al. [15], integrating the thermal capacitance of the heat carrier fluid and pipe and later improved by Pasquier and Marcotte [16]. In addition, short-term analytical solutions have also been developed, for example the one developed by Li and Lai [19], which can be used in time scales greater than one hour (up to several years), but not in very short-term scales (in the range of minutes) needed to reproduce the dynamic behaviour of an on/off GSHP; or the short-term analytical solution developed by Javed and Claesson [20], who studied the BHE heat transfer and the boundary conditions in the Laplace domain by using a thermal network, but also developing a numerical solution.

Apart from these models, there also exist some other computer programs that can be used in order to assist in the design and simulation of GSHP systems and BHEs. Among them, GLHEPRO[21], EED[22], EnergyPlus[23] or TRNSYS[24]. In order to simulate the behaviour of, not only the BHE itself, but the entire GSHP system and the coupling between the different components, a transient simulation program (like TRNSYS) is a powerful tool, since it is able to connect the models of the different components and solve the simultaneous equations of the system model, displaying the results[25]. It is possible to find several BHE models already implemented in TRNSYS, two of the most commonly used are the Superposition Borehole Model (SBM), developed by Eskilson[26,27] and implemented in TRNSYS by Pahud[28,29]; and the Duct Storage model (DST), developed by Hellström[30,31] and implemented in TRNSYS by Pahud[32,33]. The main drawback of these models is that they neglect the heat capacity of the fluid and the grout existing in the BHE, and show a low accuracy during the short-term injection period[34].

In this context, the B2G dynamic model [35,36] was developed for a U-tube Borehole Heat Exchanger (BHE) configuration and implemented in TRNSYS environment. This model consists of a thermal resistance and capacity model and has been validated against experimental data. It is able to predict with high accuracy (absolut error within 0.15K) the short-term behaviour of a U-tube BHE and also the long-term response of the ground when it is coupled with a long-term model, as the g-function model [37].

In this work, the new upgraded B2G dynamic model adapted to a standard coaxial BHE configuration and then implemented in TRNSYS is presented and described. The novelty of this upgraded version relies on the improvement of the modelling of the surrounding ground in order to be able to accurately reproduce the very short-term, short-term and mid-term behaviour of the BHE with a low computational cost. For this purpose, several new features were included. Among them, the vertical heat transfer in the ground and grout, different thermal properties in a heterogeneous layered ground, the use of three ground nodes, instead of only one (that was considered in the former version of the U-

tube B2G), to accurately model the short-mid term behaviour of the local surrounding ground. For a widespread use of this B2G new upgraded model, these three ground nodes were obtained by means of polynomial correlations, which determine their optimal location for any type of ground, geometry and operating conditions. Thus, enhancing the widespread use of the B2G model among the research community and other stakeholders in GSHP applications.

A preliminar version of the upgraded B2G model was experimentally validated and presented in [38,39] for a standard coaxial configuration, as well as was for an innovative coaxial configuration with spiral flow inside the framework of the GEOTeCH project [39–41]. This preliminar version only had two ground nodes and it did not include the optimal ground nodes determination as part of the model.

This research work presents the complete final version of the new upgraded B2G model as well as its experimental validation using the monitored data from an installation located in Tribano (Padua, Italy), under normal operating conditions. For this purpose, different days have been selected, accounting for summer and winter periods, as well as several following days. The simulated results show a good agreement with the experimental data, with a Root Mean Square Error (RMSE) lower than 0.08 K for a winter day, lower than 0.09 K for 5 days in winter and around 0.12 K for a summer day. The difference in the calculated heat transfer is lower than 4% in all the cases.

2 B2G model

The B2G (Borehole-to-Ground) model was originally developed to predict the thermal interaction between a BHE and the surrounding ground, focused on the short-term evolution of the fluid temperature. It is based on a thermal network approach together with a vertical discretization of the BHE in a way that the radial heat transfer between the different parts of the borehole (fluid inside the pipes, grout and ground) is modelled by a 2D thermal network at each depth. The advection of the fluid is modelled, so the vertical temperature distribution is calculated. In order to reproduce the thermodynamics of the fluid with a computational cost as low as possible, the simplest thermal network that is able to reproduce the BHE behaviour with accuracy enough (RMSE < 0.1K) was used. For this purpose, only the portion of surrounding ground that is affected by the heat injection/extraction period is considered in the thermal network.

The thermal network consists of different nodes, representing each part of the BHE and considering their thermal properties. The thermal interaction between nodes is calculated by the use of thermal resistances. These thermal resistances model the conductive and convective heat transfer between the different parts involved. Furthermore, the thermal inertia of the fluid, the grout and the ground is represented by a thermal capacitance in each node.

2.1 U-tube B2G model

The B2G model was initially created for a single U-tube BHE configuration and previously presented, together with its experimental validation under different conditions [35,36]. The 2D thermal network consists of five thermal capacitances and six thermal resistances, forming a 5C6R-*n* model, where *n* is the number of vertical divisions. This system can be solved numerically, solving the system of ordinary differential equations[35]. The thermal network is presented in Figure 1, where T_1 and T_2 represent the upward and downward fluid inside the pipe, T_{b1} and T_{b2} represent the grout (it is divided in two regions) and T_g represents the surrounding ground affected by the heat injected/extracted in the daily working period of the BHE.

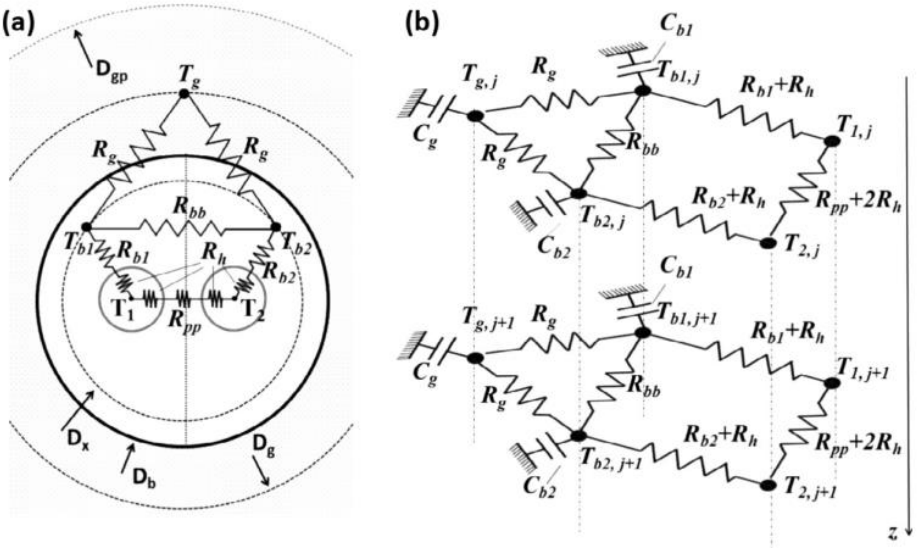

Figure 1. Thermal network model adopted: (a) 2D model; (b) 3D model [35].

The vertical conduction (axial transport) is neglected, but the fluid advection in the vertical direction is taken into account in the transient energy balance equations.

The model was able to calculate the short-term behaviour of different BHEs with a high accuracy (absolut error within 0.15°C) under different conditions [35,36], as well as predicting the dynamic behaviour of a BHE during the operation of a GHSP facility when coupled with a long-term BHE model, as the g-function model [37].

2.2 Coaxial B2G model

In order to obtain a new coaxial BHE model, and aid in the design and the operation of a GSHP system with this kind of BHEs, the B2G model was adapted to a standard coaxial BHE. A first approach to this configuration was previously presented [38,39], as well as the approach to a coaxial helical configuration [39–41]. In this work, the thermal network has been extended in order to include three ground nodes: close ground (ground node 1), further ground (ground node 2) and undisturbed ground (undisturbed ground node). In addition, a new methodology for the calculation of the ground nodes position has been used.

The new thermal network consists of five nodes with their five thermal capacitances; together with an additional node, that represents the undisturbed ground (therefore, presenting an infinite capacitance and constant temperature). Each node represents one part of the BHE: T_i represents the fluid flowing inside the inner pipe, T_o represents the fluid in the outer pipe, T_b represents the grout of the borehole, T_{g1} represents the first ground node, T_{g2} represents the second ground node and T_{ug} represents the undisturbed ground node. In this model, three ground nodes are used instead of only one (as in the U-tube B2G model). With these three ground nodes, it is possible to have a higher accuracy of the BHE thermal response during the different heat injection periods, without greatly incrementing the complexity of the model:

- The first ground node (T_{g1}) represents the closer ground region in contact with the borehole, which has a higher influence in the short-term response of the BHE.
- The second ground node (T_{g2}) represents the further ground region, with a lower influence in the short-term response but a higher influence in the mid-term response.

- The undisturbed ground node (T_{ug}) represents the far surrounding ground, which keeps a constant temperature, as it remains undisturbed during the heat injection period assumed in the model.

The convective and conductive heat transfer between the different nodes was calculated by the use of radial thermal resistances between nodes (R_{io}, R_{ob}, R_{bg1}, R_{g1g2} and R_{g2ug}). The heat conduction between the vertically adjacent grout and ground nodes has also been considered by the use of vertical thermal resistances (R_{vb}, R_{vg1} and R_{vg2}).

This thermal network is depicted in Figure 2, while the vertical discretization of the BHE is shown in Figure 3.

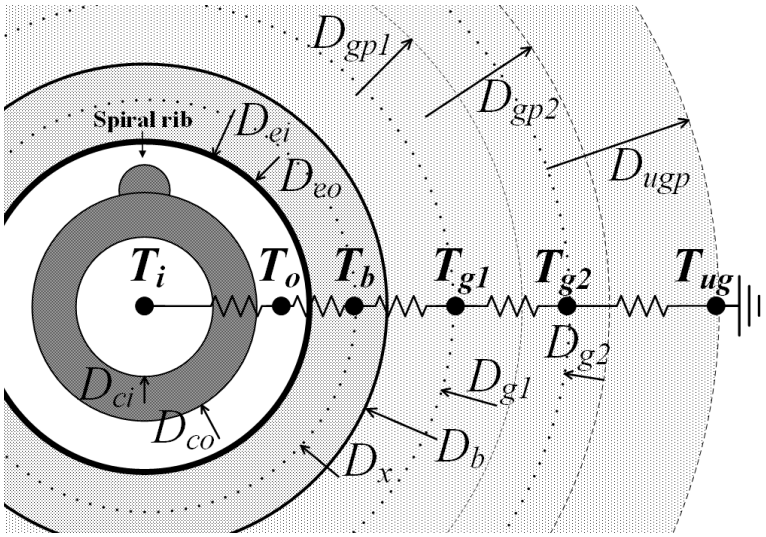

Figure 2. Thermal network of the coaxial configuration model: borehole layout

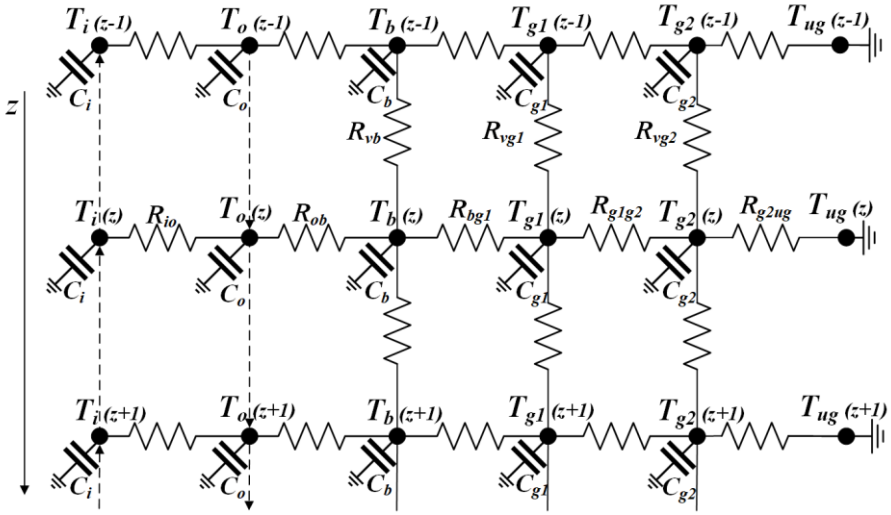

Figure 3. Thermal network of the coaxial configuration model: vertical discretization

The energy balance equations composing the system are described in the following:

- For the fluid nodes, the axial heat conduction is neglected, but the advection in the vertical direction is considered. In the case of the fluid inside the inner pipe, the transient energy balance equation will consider not only the vertical advection (represented by its vertical velocity, v_i),

but also the heat exchange with the fluid in the outer pipe (equation (1)). In the case of the fluid inside the outer pipe, the transient energy balance equation will consider its vertical advection (v_o) and also the heat exchange with the fluid in the inner pipe and the grout (Equation (2)).

$$\frac{\partial T_i(z)}{\partial t} = v_i \frac{\partial T_i(z)}{\partial z} - \frac{1}{C_i}\left(\frac{T_i(z) - T_o(z)}{R_{io}}\right) \tag{1}$$

$$\frac{\partial T_o(z)}{\partial t} = -v_o \frac{\partial T_o(z)}{\partial z} - \frac{1}{C_o}\left(\frac{T_o(z) - T_i(z)}{R_{io}} + \frac{T_o(z) - T_b(z)}{R_{ob}}\right) \tag{2}$$

- For the grout node, the heat exchange with the adjacent nodes in the same vertical depth is considered (fluid inside the outer pipe and first ground node), but also the vertical heat exchange between the vertically adjacent grout nodes (at the depths immediately above and below), as shown in equation (3).

$$C_b \frac{\partial T_b(z)}{\partial t} = \frac{T_o(z) - T_b(z)}{R_{ob}} + \frac{T_{g1}(z) - T_b(z)}{R_{bg1}} + \frac{T_b(z-1) - T_b(z)}{R_{vb}} + \frac{T_b(z+1) - T_b(z)}{R_{vb}} \tag{3}$$

- For the first and second ground nodes, the heat exchange with the adjacent nodes in the same vertical depths is considered, as well as the vertical heat conduction with the vertically adjacent nodes, as shown in equations (4) and (5).

$$C_{g1} \frac{\partial T_{g1}(z)}{\partial t} = \frac{T_b(z) - T_{g1}(z)}{R_{bg1}} + \frac{T_{g2}(z) - T_{g1}(z)}{R_{g1g2}} + \frac{T_{g1}(z-1) - T_{g1}(z)}{R_{vg1}} + \frac{T_{g1}(z+1) - T_{g1}(z)}{R_{vg1}} \tag{4}$$

$$C_{g2} \frac{\partial T_{g2}(z)}{\partial t} = \frac{T_{g1}(z) - T_{g2}(z)}{R_{g1g2}} + \frac{T_{ug}(z) - T_{g2}(z)}{R_{g2ug}} + \frac{T_{g2}(z-1) - T_{g2}(z)}{R_{vg2}} + \frac{T_{g2}(z+1) - T_{g2}(z)}{R_{vg2}} \tag{5}$$

- The undisturbed ground node is assumed to maintain the far-field temperature (undisturbed ground temperature) at each depth: $T_{ug}(z,t) = T_\infty(z)$.

2.3 Parameter Calculation

The main parameters of the model are the thermal capacitances and the thermal resistances, which can be determined based on the thermo-physical properties and the geometrical characteristics of the borehole. Furthermore, it is possible to consider different thermo-physical properties (thermal conductivity and thermal capacity) for the grout and ground at different depths in a heterogeneous layered ground. Therefore, the thermal resistances and thermal capacitances may be different at different depths.

2.3.1 Thermal Capacitances

The thermal capacitances (C) are calculated considering the volumetric thermal capacitance at the corresponding depth (c) and the volume of the zone in each vertical division (dz). The grout and ground capacitances are calculated according to Eqs.(6), where D_b represents the borehole diameter and D_{eo} represents the external diameter of the outer pipe.

$$C_{g1} = \frac{\pi}{4}\left(D_{gp1}^2 - D_b^2\right) c_g dz \quad ; \quad C_{g2} = \frac{\pi}{4}\left(D_{gp2}^2 - D_{gp1}^2\right) c_g dz \quad ; \quad C_b = \frac{\pi}{4}(D_b^2 - D_{eo}^2)\, c_b\, dz \quad (6)$$

The thermal capacitance of the fluid nodes is calculated based on the fluid heat capacity (C_p), the fluid density (ρ) and the volume, according to Equation(7). Here, D_{ci} represents the inner diameter of the inner pipe, D_{ei} represents the inner diameter of the outer pipe and D_{co} represents the outer diameter of the inner pipe.

$$C_i = \frac{\pi}{4} D_{ci}^2\, C_{p,i}\, \rho_i dz \quad ; \quad C_o = \frac{\pi}{4}(D_{ei}^2 - D_{co}^2)\, C_{p,o}\, \rho_o dz \quad (7)$$

All the fluid properties (heat capacity (C_p), density (ρ), dynamic viscosity (μ) and thermal conductivity (λ)) are calculated according to the correlations presented in [42], depending on the temperature of the fluid, the type of fluid (water or MPG and water mixture) and in the second case, the percentage of MPG in the mixture.

2.3.2 Thermal resistances

Thermal resistances are calculated as an addition of conductive and convective cylindrical thermal resistances. For the calculation of the conductive resistance, the nodes are located at an equivalent diameter. The equivalent diameter is calculated as the mean diameter of the zone according to Equation (8), where D_x is the grout node diameter, D_{g1} corresponds to the short-term node diameter and D_{g2} corresponds to the mid-term node diameter.

$$D_x = \frac{D_b + D_{eo}}{2} \quad ; \quad D_{g1} = \frac{D_{gp1} + D_b}{2} \quad ; \quad D_{g2} = \frac{D_{gp2} + D_{gp1}}{2} \quad (8)$$

Regarding the convective thermal resistance, it is calculated using the average convective heat transfer coefficient (h) of the fluid in the inner pipe (h_i) and in the outer pipe (h_o), using Equation (9). The thermal conductivity of the fluid is represented by k, and the Nusselt number (Nu) is calculated depending on the flow regime (laminar or turbulent) and the geometrical configuration (circular tube in the inner pipe and concentric annular in outer pipe) [43]. These properties are calculated at the average temperature of the fluid inside each pipe (inner or outer pipe).

$$h = \frac{Nu\, k}{D} \quad (9)$$

The internal diameter is considered in the inner pipe (D_{ci}). Regarding the outer pipe, it is considered an equivalent hydraulic diameter ($D_h = D_{ei} - D_{co}$).

Concerning the conductive thermal resistances, they are calculated considering the conductivities of the inner pipe (k_{ip}), the outer pipe (k_{op}), the grout (k_b) and the ground (k_g) at the corresponding depth. The total thermal resistances between the different nodes in the thermal network are described in Eqs. (10) -(14).

$$R_{io} = \frac{1}{\pi\, D_{ci}\, dz\, h_i} + \frac{\ln(D_{co}/D_{ci})}{2\,\pi\, k_{ip}\, dz} + \frac{1}{\pi\, D_{co}\, dz\, h_o} \quad (10)$$

$$R_{ob} = \frac{1}{\pi\, D_{ei}\, dz\, h_o} + \frac{\ln(D_{eo}/D_{ei})}{2\,\pi\, k_{op}\, dz} + \frac{\ln(D_x/D_{eo})}{2\,\pi\, k_b\, dz} \tag{11}$$

$$R_{bg1} = \frac{\ln(D_b/D_x)}{2\,\pi\, k_b\, dz} + \frac{\ln\left(D_{g1}/D_b\right)}{2\,\pi\, k_g\, dz} \tag{12}$$

$$R_{g1g2} = \frac{\ln\left(D_{g2}/D_{g1}\right)}{2\,\pi\, k_g\, dz} \tag{13}$$

$$R_{g2ug} = \frac{\ln\left(D_{ug}/D_{g2}\right)}{2\,\pi\, k_g\, dz} \tag{14}$$

Regarding the vertical thermal resistances between adjacent nodes, they are calculated according to Eqs (15)-(16), depending on the thermal conductivity at the corresponding depth, the vertical distance between nodes (dz) and the annulus surface. The thermal conductivity considered is the same in the vertical and radial direction.

$$R_{vb} = \frac{dz}{\frac{\pi}{4}\cdot\left(D_b^2 - D_{eo}^2\right)\cdot k_b} \tag{15}$$

$$R_{vg1} = \frac{dz}{\frac{\pi}{4}\cdot\left(D_{gp1}^2 - D_b^2\right)\cdot k_g} \quad ; \quad R_{vg2} = \frac{dz}{\frac{\pi}{4}\cdot\left(D_{gp2}^2 - D_{gp1}^2\right)\cdot k_g} \tag{16}$$

2.3.3 Numerical resolution

The energy balance equations (1)-(5) can be implemented in any simulation software once the parameters have been calculated. In order to solve the system, it is necessary to solve the equations numerically. In this work, the Lax-Wendroff method [44] has been used. In this way, the temperatures of each node of the thermal network are calculated at a certain time (*t+1*), considering the temperature values at the previous instant (*t*), for each vertical section of the borehole (*j*), according to the Eqs. (17)-(21). Where *j=1* represents the surface of the borehole and *j=n* represents the bottom of the borehole.

$$\begin{aligned} T_i^{t+1}(j) = T_i^t(j) + \frac{\Delta t\; v_i}{2\; dz}\left(\left(T_i^t(j+1) - T_i^t(j-1)\right) + \frac{\Delta t\; v_i}{dz}\left(T_i^t(j+1) - 2\,T_i^t(j) + T_i^t(j-1)\right)\right) \\ - \frac{\Delta t}{C_i}\left(\frac{T_i^t(j) - T_o^t(j)}{R_{io}}\right) \end{aligned} \tag{17}$$

$$\begin{aligned} T_o^{t+1}(j) = T_o^t(j) - \frac{\Delta t\; v_o}{2\; dz}\left(\left(T_o^t(j+1) - T_o^t(j-1)\right) - \frac{\Delta t\; v_o}{dz}\left(T_o^t(j+1) - 2\,T_o^t(j) + T_o^t(j-1)\right)\right) \\ - \frac{\Delta t}{C_o}\left(\frac{T_o^t(j) - T_i^t(j)}{R_{io}} + \frac{T_o^t(j) - T_b^t(j)}{R_{ob}}\right) \end{aligned} \tag{18}$$

$$T_b^{t+1}(j) = T_b^t(j) + \frac{\Delta t}{C_b}\left(\frac{T_o^t(j) - T_b^t(j)}{R_{ob}} + \frac{T_{g1}^t(j) - T_b^t(j)}{R_{bg1}} + \frac{T_b^t(j-1) - T_b^t(j)}{R_{vb}} + \frac{T_b^t(j+1) - T_b^t(j)}{R_{vb}}\right) \tag{19}$$

$$T_{g1}^{t+1}(j) = T_{g1}^{t}(j) + \frac{\Delta t}{C_{g1}}\left(\frac{T_b^t(j) - T_{g1}^t(j)}{R_{bg1}} + \frac{T_{g2}^t(j) - T_{g1}^t(j)}{R_{g1g2}} + \frac{T_{g1}^t(j-1) - T_{g1}^t(j)}{R_{vg1}} + \frac{T_{g1}^t(j+1) - T_{g1}^t(j)}{R_{vg1}}\right) \quad (20)$$

$$T_{g2}^{t+1}(j) = T_{g2}^{t}(j) + \frac{\Delta t}{C_{g2}}\left(\frac{T_{g1}^t(j) - T_{g2}^t(j)}{R_{g1g2}} + \frac{T_{ug} - T_{g2}^t(j)}{R_{g2ug}} + \frac{T_{g2}^t(j-1) - T_{g2}^t(j)}{R_{vg2}} + \frac{T_{g2}^t(j+1) - T_{g2}^t(j)}{R_{vg2}}\right) \quad (21)$$

In these equations, Δt represents the time-step used for the calculations. This value should be lower than the maximum fixed by the Courant-Friedrichs-Lewy (CFL) condition. This condition should be fulfilled in order to assure that the fluid displacement in the time-step is lower than the distance between nodes, according to the equation (22), where dz represents the vertical division length and v the fluid velocity inside the pipe.

$$\frac{\Delta t}{\Delta t_{MAX}} = CFL \leq 1\,; \quad \Delta t_{MAX} = \frac{dz}{v} \quad (22)$$

Therefore, if the time-step of the simulation is greater than the maximum value Δt_{MAX}, the internal time-step in the BHE model (Δt) will be subdivided into smaller time-steps that satisfy the CFL condition. For this purpose a maximum value of $CFL = 0.99$ is fixed, assuring a small error margin, and the minimum Δt_{MAX} is calculated, considering the velocity of the fluid in the inner pipe (v_i) and in the outer pipe (v_o). Then, the internal time-step is calculated as expressed in the equation (23):

$$\Delta t = 0.99 \cdot \min\left(\frac{dz}{v_i}, \frac{dz}{v_o}\right) \quad (23)$$

2.4 Optimal location of the ground nodes

Regarding the thermal response of the ground and the amount of soil that is affected by the heat injection during a specific time period, it is usually addressed by adding a number of radial ground nodes and discretizing the soil mass in small radial steps until the far-field radius, where the effect of the heat injection vanishes. This far-field radius calculation has been addressed by several authors, for example, Hart and Couvillion [45] defined it as $r_\infty = 4\sqrt{\alpha t}$, which depends on the ground thermal diffusivity (α) and the injection period (t). The addition of ground nodes inevitably leads to an increase in the complexity of the model and therefore, an increase in the computational cost. Therefore, only three ground nodes are used in the coaxial B2G model in order to model the affected surrounding ground. In this context, the location of the ground nodes position is key in order to accurately reproduce the thermal behaviour of the surrounding ground affected by the heat exchange with the BHE.

The position of the three ground nodes is defined by three penetration radii: R_{gp1} for the first ground node (short-term), R_{gp2} for the second ground node (mid-term) and R_{ug} for the undisturbed ground node. The calculation of these penetration radii is not straightforward, as they will influence in the calculation of the ground temperature and thus, in the fluid temperature calculation. For example, for the first ground node, the higher the value of the penetration radius, the greater the amount of ground that the model will consider, and as a consequence, the greater will be the heat capacity of this ground section. In the case of a greater heat capacity, the temperature of this node will vary more slowly, and it will have an influence on the short-term evolution of the water temperature. Analogously, the same will occur with the second ground node. However, the position of the undisturbed ground node will

only have an influence in the heat transfer between the second ground node and the undisturbed ground node (increasing or decreasing the thermal resistance), as it only represents a temperature boundary, with no temperature variation.

The optimal position of the three ground nodes will depend on the thermo-physical properties of the ground (effective thermal conductivity and capacity), the operating conditions (heat injection period in a day) and the borehole geometry (borehole diameter), according to the equation (24). In the determination of the effective thermal conductivity and capacity the weighted average of the different layers has been calculated in the case of a layered ground with different materials; in the case of groundwater flow, an increased thermal conductivity would be considered to account for this effect.

$$R_{gp1}, R_{gp2}, R_{ug} = f(k_g, c_g, t, D_b) \tag{24}$$

In the B2G model thermal network, the ground nodes position was defined by the penetration diameters. These diameters are defined by the penetration radii, as it is presented in the equation (25).

$$D_{gp1} = 2 \cdot R_{gp1}\,; \quad D_{gp2} = 2 \cdot R_{gp2}\,; \quad D_{ug} = 2 \cdot R_{ug} \tag{25}$$

2.4.1 Methodology

In order to calculate the optimal location of the ground nodes that reproduces with the highest possible accuracy the temperature variation of the ground nodes and the heat transfer along the ground, a new methodology is proposed and described in [46]. It consists in comparing the B2G model with the Infinite Cylindrical Source (ICS) model, trying to minimize the difference between the results of the two models when calculating the temperature of the first and second ground nodes.

In this comparison, a constant heat flux on the borehole wall during all the heat injection period is assumed, and the ground temperature variation is calculated for the ground nodes position and the heat transfer rate between them, for each time step. The ground nodes position (penetration radii R_{gp1}, R_{gp2} and R_{ug}; corresponding to the ground nodes T_{g1}, T_{g2} and T_{ug}, respectively) will be optimized, so the difference between the results calculated by the two models is minimum.

For this purpose, the B2G thermal network has been adapted in order to consider a constant heat flux on the borehole wall instead of the fluid through the BHE tubes. Therefore, a node on this surface is considered (T_b), and a constant heat flux (q_0) is imposed. Figure 4 shows the thermal network corresponding to this problem. The ground nodes T_{g1} and T_{g2} are located, each one, at the average distance between the two concentric circumferences that form each annulus region. These positions are defined by the radii r_{g1} and r_{g2}, respectively, according to the equation (26).

$$r_{g1} = \frac{R_{gp1} + r_b}{2} \quad ; \quad r_{g2} = \frac{R_{gp2} + R_{gp1}}{2} \tag{26}$$

where r_b represents the borehole wall radius. On the other hand, q_1 represents the heat transfer between the ground nodes T_{g1} and T_{g2}, while q_2 represents the heat transfer between T_{g2} and T_{ug}.

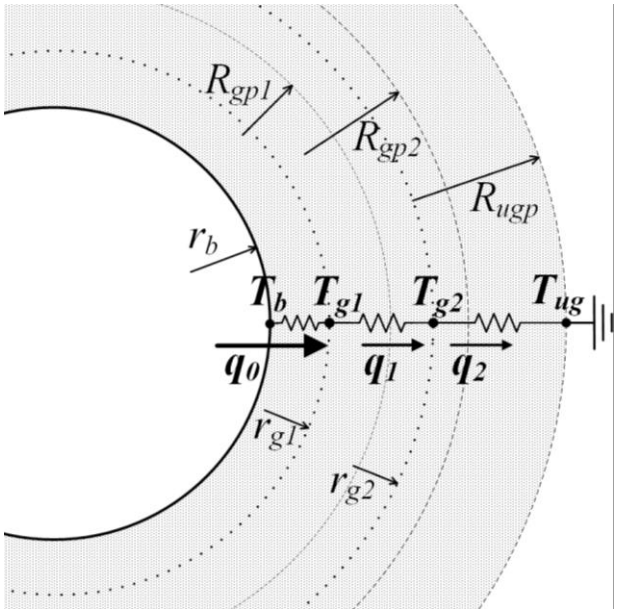

Figure 4. Thermal network used for the calculation of the penetration radii

The main parameters used in the models are the borehole radius (r_b), the ground thermal conductivity (λ), the ground volumetric heat capacity (c_v) and the heat flux (q_0). The main inputs are the three penetration radii (R_{gp1}, R_{gp2} and R_{ug}). The initial ground temperature is assumed to be zero, as only the temperature variation is calculated.

An optimization algorithm implemented in MATLAB® is used to find the optimal position of the three ground nodes that minimizes the difference between the B2G and the ICS models. Finally, in order to make the use of the B2G more general, polynomial correlations will be calculated to define these ground nodes positions and implemented inside the TRNSYS B2G model, so the position of the ground nodes can be calculated internally depending on the soil thermal properties, the BHE geometry and the system operating conditions. This way, the use of the B2G model can be extended to any BHE configuration, type of soil and operating conditions (total equivalent daily operating hours), enhancing its widespread use, as the user only needs to introduce these parameters as inputs to the TRNSYS type instead of estimating the ground penetration diameters. Furthermore, this methodology can be implemented for the U-tube B2G model, as the penetration diameters are calculated considering the heat injection on the borehole wall.

2.4.1.1 B2G model

In the B2G model, the temperature of the ground nodes T_{g1} and T_{g2} is calculated using the main BHE parameters and penetration radii. First, the thermal capacitances (C) of the two ground nodes are calculated according to equation (27), together with the UA values, which represent the thermal resistance between ground nodes, as shown in equation (28).

$$C_{g1} = \pi \left(R_{gp1}^2 - r_b^2\right) c_v \quad ; \quad C_{g2} = \pi \left(R_{gp2}^2 - R_{gp1}^2\right) c_v \tag{27}$$

$$UA_{bg1} = \frac{2\,\pi\,\lambda}{\ln\left(r_{g1}/r_b\right)} \; ; \quad UA_{g1g2} = \frac{2\,\pi\,\lambda}{\ln\left(r_{g2}/r_{g1}\right)} \; ; \quad UA_{g2ug} = \frac{2\,\pi\,\lambda}{\ln\left(R_{ug}/r_{g2}\right)} \tag{28}$$

Second, the ground nodes temperatures (T_{g1} and T_{g2}) are calculated using the energy balance equations. The undisturbed ground temperature is defined as zero ($T_{ug} = 0$).

$$C_{g1}\frac{\partial T_{g1}(t)}{\partial t} = q_0 + UA_{g1g2}\left(T_{g2}(t) - T_{g1}(t)\right) \tag{29}$$

$$C_{g2}\frac{\partial T_{g2}(t)}{\partial t} = UA_{g1g2}\left(T_{g1}(t) - T_{g2}(t)\right) + UA_{g2ug}\left(T_{ug}(t) - T_{g2}(t)\right) \tag{30}$$

2.4.1.2 Infinite Cylindrical Source model

The Infinite Cylindrical Source (ICS) model calculates the heat transfer in the region bounded internally by a hollow circular cylinder and constant heat flux in its surface. In this case, the internal circular cylinder would correspond to the BHE, with radius r_b, and the constant heat flux through its surface would be q_0. The solution for the calculation of the ground temperature along the radial distance was provided by Carslaw and Jaeger [10]. This solution is presented in equation (31), where the initial ground temperature is zero, and α represents the thermal diffusivity of the ground ($\alpha = \lambda/c_v$).

$$T^{ICS}(r,t) = -\frac{q_0}{\pi^2 r_b \lambda}\int_0^{\infty}\left(1 - e^{-\alpha u^2 t}\right)\frac{J_0(ur)\,Y_1(ur_b) - Y_0(ur)\,J_1(ur_b)}{u^2\left[J_1^2(ur_b) + Y_1^2(ur_b)\right]}du \tag{31}$$

Therefore, the temperature in the ground nodes will be calculated by the equation (32).

$$T_{g1}^{ICS}(t) = T^{ICS}\left(r_{g1}, t\right) \quad ; \quad T_{g2}^{ICS}(t) = T^{ICS}\left(r_{g2}, t\right) \tag{32}$$

2.4.2 Calculation of the ground nodes position

Both the B2G and ICS models were implemented in MATLAB®, so it is possible to calculate for each time step the temperature of the ground nodes and the heat transfer rates for a given set of parameters: borehole radius (r_b), ground properties (thermal conductivity, λ and volumetric heat capacity, c_v), heat flux (q_0) and heat injection time (t). The penetration radii (to be optimized) are introduced as inputs in the models: R_{gp1}, R_{gp2} and R_{ug}.

In order to compare the two models, the temperatures of the first and second ground nodes (T_{g1} and T_{g2}, respectively) are calculated by each model. So, the optimization solver will calculate the set of radii that minimizes the RMSE between these temperatures, calculated by the B2G and the ICS models. The total RMSE is defined as the sum of the RMSEs for each temperature, as shown in the equation (33).

$$\sum RMSE = \sqrt{\frac{\sum_{i=1}^{t}\left(T_{g1,i}^{B2G} - T_{g1,i}^{ICS}\right)^2}{n}} + \sqrt{\frac{\sum_{i=1}^{t}\left(T_{g2,i}^{B2G} - T_{g2,i}^{ICS}\right)^2}{n}} \tag{33}$$

In order to find the optimal penetration radii, an optimization algorithm is used. For this study, a pattern search optimization methodology was used, using the solver *patternsearch* already implemented in the Global Optimization Toolbox in MATLAB® [47]. In this solver, initial values for the penetration radii are provided, and it will search the values of the radii that minimize the sum of RMSEs ($\sum RMSE$), subject to the constraint that each ground node penetration radius must be lower than the next one, according to the equation (34).

$$R_{gp1} < R_{gp2} < R_{ug} \tag{34}$$

The new methodology was tested for a real BHE using data from a Thermal Response Test (TRT) carried out in Houten, The Netherlands [46]. However, in order to facilitate this calculation for any type of soil, BHE and system operating conditions, a parametric calculation was carried out for a wide range of values of the different variables in order to obtain a polynomial correlation, easy to handle, to be implemented inside the B2G model. Therefore, it can automatically calculate the ground nodes position, introducing the values of the influencing variables as inputs. The values that were used for the parametric study are shown in Table 1.

Table 1. Parameters values to calculate the penetration radii correlations

Parameter	Values	Units
Ground thermal conductivity (λ)	[1 2 3 4]	$W/(m \cdot K)$
Ground volumetric heat capacity (c_v)	[1000 2000 3000 4000]	$kJ/(m^3 \cdot K)$
Borehole radius (r_b)	[0.03 0.05 0.07 0.09]	m
Heat injection time during one day (t)	[6 12 18 24]	h

It should be mentioned that the calculation of the ground nodes position was carried out with different values of heat flux, q_0 (15, 30 and 90 W/m), producing the same optimal position of the ground nodes. Therefore, it can be concluded that this position is independent of the heat injected, but only depends on the parameters mentioned above. As a consequence, this optimal position will be valid when used inside the B2G model for a variable heat load in the BHE, also along the borehole depth. So it can be used for the modelling of a whole ground source heat pump system, where the heat load into the ground will vary.

A combination of the different parameters shown in Table 1 was used as an input to the MATLAB® optimization method, considering a time step (Δt) of 1 minute. Several preliminar studies were carried out in order to find an appropriate expression that better correlates the different parameters in a single equation for each penetration radius. The optimization algorithm implies difining an initial point. As a first approach, different initial points in the algorithm ($[R_{gp1_0}\ R_{gp2_0}\ R_{ug_0}]$ = [0.1 0.2 0.3] m and $[R_{gp1_0}\ R_{gp2_0}\ R_{ug_0}]$ = [0.3 0.6 0.8] m) were defined for the penetration radii. It was found that an expression that fitted with a good accuracy the calculated points is one correlating each penetration radius divided by the borehole radius as a function of the Fourier number (using the borehole radius as the representative length), as shown in the equations (35)-(38).

$$\frac{R_{gp1}}{r_b} = A_1 + B_1 \cdot Fo_b^{C_1} \tag{35}$$

$$\frac{R_{gp2}}{r_b} = A_2 + B_2 \cdot Fo_b^{C_2} \tag{36}$$

$$\frac{R_{ug}}{r_b} = A_{ug} + B_{ug} \cdot Fo_b^{C_{ug}} \tag{37}$$

$$Fo_b = \frac{\alpha \cdot t}{r_b^2} \tag{38}$$

where A_i, B_i, C_i are constants to be calculated, α is the ground thermal diffusivity, t is the heat injection time and r_b is the borehole radius.

Once the type of correlation is identified (equations (35)-(37)), it can be used to better define the initial points of the penetration radii [R_{gp1_0} R_{gp2_0} R_{ug_0}] in the optimization algorithm. In Figure 5, it is shown the preliminary results obtained with the MATLAB® algorithm, used to obtain the preliminary correlations for setting this initial point. Considering the coefficients presented in Table 2 in the equations (35)-(37), it is possible to provide initial points for the different combination of variables, closer to the global optimum, rather than using a constant starting point for all the values of the parameters as it was initially carried as a first approach. Therefore, it was decided to use these preliminary correlations to set the initial points in the optimization algorithm in MATLAB®, for the determination of the final correlations.

Table 2. Coefficients of the preliminary correlations used as initial point [48]

	R_{gp1_0}	R_{gp2_0}	R_{ug_0}
A_i	1.268325	0.663032	0.922542
B_i	0.482196	1.621079	2.265936
C_i	0.502414	0.470611	0.487034

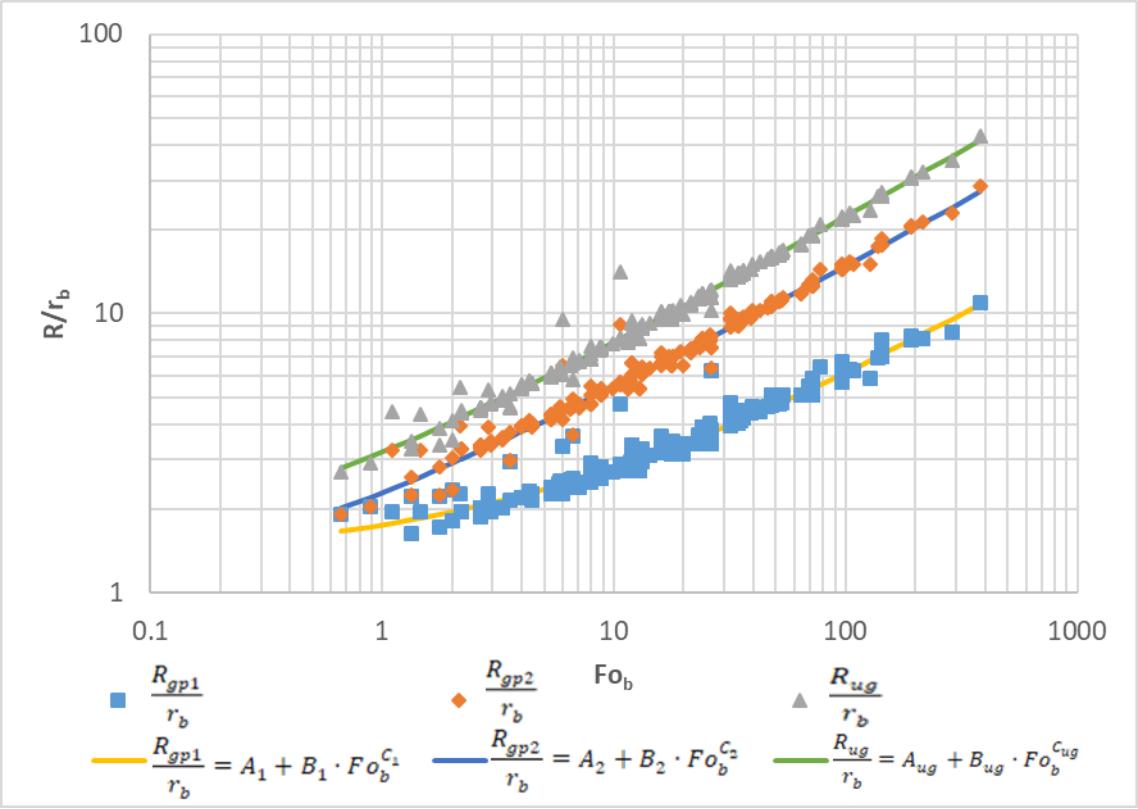

Figure 5. Preliminary correlations for setting the intial point [R_{gp1_0} R_{gp2_0} R_{ug_0}]

The results of the final parametric study are shown in Figure 6 (plotted markers), together with the values obtained with the final correlations (plotted in solid lines). The coefficients of these correlations are shown in Table 3.

Table 3. Calculated coefficients for the final penetration radii correlations

	R_{gp1}	R_{gp2}	R_{ug}
A_i	0.976794	0.926305	0.767003
B_i	0.611236	1.416714	2.312549
C_i	0.420103	0.451364	0.466674

Figure 6 shows that the correlations fit with a good accuracy the calculated points, the RMSE for each of the penetration radii correlation was calculated, comparing the values of the 256 points calculated by the optimization algorithm with the values calculated with each correlation, obtaining a RMSE of 0.0017 m for R_{gp1}, 0.0049 m for R_{gp2} and 0.0077 m for R_{ug}. So the correlations calculate with a good accuracy the penetration radii and are fitted to be used inside the B2G model.

The polynomial correlations were implemented inside the B2G model in order to automatically calculate the penetration radii that define the ground nodes positions. The suitability of these correlations will be proved in the following section, where the whole B2G model will be experimentally validated.

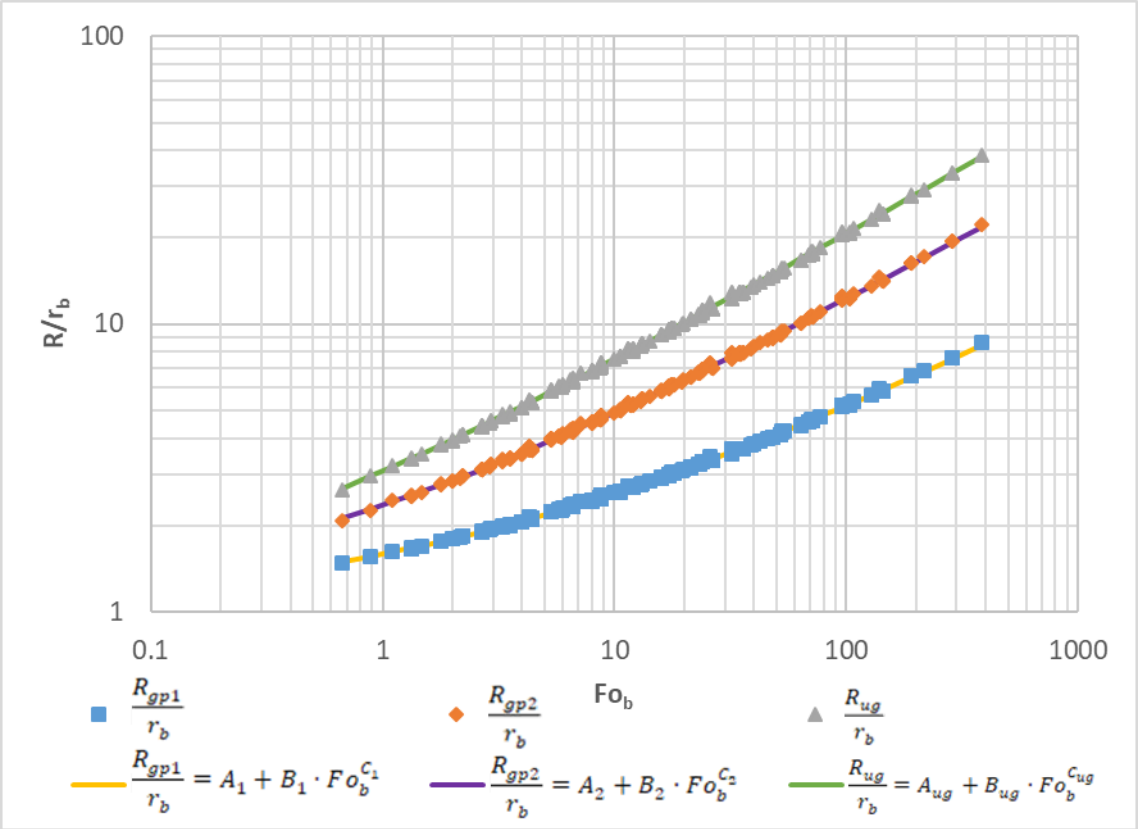

Figure 6. Comparison between the penetration radii correlations and calculated points

3 Experimental validation

3.1 Installation in Tribano

In this work, experimental measurements under the normal operation of a demonstration installation in Tribano have been used to validate the BHE model. The Tribano demo-site is one of the demonstration facilities installed in the framework of the H2020 European project GEOTeCH [49], located at the factory of the company HiRef S.p.A. [50] in the municipality of Tribano, in the province of Padua (Italy). It consists of a Dual Source Heat Pump (DSHP) system, able to work with the ground or the air as a source/sink. It provides heating and cooling to four rooms in the office building located at the factory. It is able to produce DHW as well. The DSHP system was installed in the second half of the year 2017 and it started working around January 2018. The DSHP installed in the system is a prototype developed inside the framework of the GEOTeCH project by HiRef S.p.A., with a nominal capacity of 16 kW for heating and 14 kW for cooling. The heat pump is located outside of the building and connected to the BHEs field 20 m far from the heat pump. The BHEs field consists of eight coaxial BHEs with a length of 30 m each. The DHW tank, the distribution of the pipes, as well as the control and data acquisition system are located inside a technical room next to the DSHP. The system is fully monitored since the beginning.

3.1.1 BHEs field

The BHEs field is located around 20 m far from the DSHP under the parking of the factory. It consists of eight coaxial BHEs with a length of 30 m each, distributed in a rectangular configuration of 2x4 with a separation of 6 m between each other (see Figure 7). The different BHEs are connected in parallel in eight different hydraulic lines, using water as the circulating fluid; the connecting pipes length to each BHE from the collector are different and the hydraulic circuit is not balanced. The water flow coming from the heat pump is distributed in the eight BHEs hydraulic lines from a collector. The BHEs present a coaxial configuration, with a PE100 SDR17 OD90 outer pipe and a PP SR11 OD63 inner pipe. The connecting pipes are PE100 SDR11 DN32. The BHEs were not grouted, as a hydrogeological study proved that it was not necessary and the hollow stem auger drilling developed in the GEOTeCH project was not equipped with the grouting devices at the moment of the installation. The absence of grouting caused the surrounding ground to collapse around each BHE when the drilling rods that contained it were removed. The geology of the site consists of unconsolidated, alluvial soil, with very fine grain size (silt and clay) and a low permeability, with sandy layers in between at different depths [51].

The eight coaxial BHEs are connected in parallel in eight different hydraulic lines that are distributed and collected in the collector pit. Since there are no balancing valves in the hydraulic system, the mass flow rate through each BHE will be different, due to the different pipes length between the collector and each BHE.

3.1.2 Monitoring system

The system incorporates a magnetic flowmeter (with an accuracy around 0.5-1.0%) in the ground loop, measuring the total mass flow rate, so there are no measurements of the flow through each BHE. As the BHEs hydraulic circuit is not balanced, the mass flow rate through each BHE might be different due to different pipe lengths. The inlet and outlet temperature of the ground loop are measured with PT100 sensors (with an expected accuracy of ± 0.1K). Additionally, some other temperature sensors

were installed in the BHE field, in order to analyse the temperature of the surrounding ground and the inlet and outlet temperatures of one of the BHEs [51]. On one hand, the inlet and outlet temperature values of BHE8 (see Figure 7) and the collector are measured with PT100 sensors. On the other hand, three observation boreholes were installed (OB1, OB2 and OB3 in Figure 7) with the purpose of studying the thermal evolution of the surrounding ground at different depths due to the climatic influence, as well as the heat injected/extracted by the BHEs. They consist of three pipes (PE100 SDR11 OD63) installed at different distances and orientations from the BHE8 in a straight line. One of them was installed between BHE8 and BHE6 (OB1), and two out of the BHEs field, west to the BHE8, at distances of 1 m (OB2) and 3 m (OB3). In this way, the thermal interaction between the two BHEs can be observed at OB1, while the OB2 and OB3 are mostly influenced only by BHE8. OB2 was installed as close to BHE8 as possible in order to study the influence of heat injection/extraction of one BHE in the local closest surrounding ground. On the contrary, the temperature measured in OB3 represents better the undisturbed ground temperature evolution.

Each observation borehole is filled with water and four temperature sensors are placed at depths of 2, 5, 10 and 15 meters each. The temperature sensors that were used are Therm Links, based on Modular Underground Monitoring System (MUMS) technology developed by ASE S.r.l. The accuracy of the Therm Links is $\pm$0.5K, and the PT100 sensors have a tolerance of 0.15K at 0°C [51].

The map with the localization of the eight BHEs, the distribution system and the monitoring boreholes OBs, is presented in Figure 7.

Figure 7. Map of the BHE field in the Tribano demo-site. Temperature sensors are located in OB 1, OB 2 and OB 3 (blue), as well as on the head of BHE8 and COL (yellow) [51]

3.2 Calculation of mass flow rates

The mass flow rate through each BHE line was estimated assuming that the total pressure drop through each line (distribution pipes and BHE) would be the same in the eight lines. So, the pressure drop was

calculated depending on the mass flow rate for the BHE and the connecting pipes. An extra pressure drop of 310 Pa was considered for the head assembly and foot inversion in the BHE, based on internal studies carried out in the GEOTHEX BHE by the company Groenholland BV [52]. The calculation of the pressure drop through each line as a function of the mass flow rate was implemented in an Excel spreadsheet and then, using the Solver tool, the mass flow rate of each line is calculated by means of a mathematical algorithm in order to obtain the same pressure loss in all the lines. The total mass flow rate that was estimated corresponds to the near constant mass flow rate at which the system was working at that moment. The solution obtained by this methodology is shown in Table 4. The flowing time through each entire line is also shown in the table. It can be seen that this time will be considerably different in the different BHE lines, because of the different length and water velocity.

Table 4. Mass flow rate calculation

BHE	Mass flow rate (kg/h)	Percentage of total flow rate	Length of one pipe (m)	Pressure drop pipes (Pa)	Pressure drop BHE (Pa)	Total pressure drop (Pa)	Flowing time (min)
1	564	14.2%	11	1272	809	2081	14
2	765	19.3%	5	1042	1039	2081	10
3	463	11.6%	17	1371	710	2081	18
4	565	14.2%	11	1274	807	2081	14
5	400	10.1%	23	1431	651	2081	21
6	463	11.6%	17	1371	710	2081	18
7	356	9.0%	29	1474	608	2081	25
8	400	10.1%	23	1431	651	2081	21
Σ	3975	100.0%				2081	

The mass flow rate through each line would be quite different depending on the length of the distribution pipes, as the pressure loss will increase with the pipe length and then, the mass flow rate will decrease in order to compensate this effect vertical discretization; as a result, the BHE lines with longer pipes would present a lower flow rate. Focusing on the BHE8, the mass flow rate would be around a 10% of the total.

For the validation of the B2G coaxial model with the BHE8 data in different days, a constant flow rate of 400 kg/h was assumed, together with the monitored inlet and outlet temperature values on the head of the BHE8.

3.3 Validation of the model under daily operating conditions

The validation of the B2G model was performed by implementing it as a new TRNSYS type. The geometrical characteristics and the thermal properties of the BHE and surrounding ground were set as parameters and the inlet temperature measured for the BHE8, together with the calculated mass flow rate were introduced as inputs in the model. Therefore, the result of the TRNSYS simulation was the outlet temperature, to be compared with the experimental values collected by the monitoring system. The RMSE between the simulated and experimental outlet temperature was calculated according to the equation (39), while the equation (40) was used to obtain the heat transfer in the fluid and then to compare the experimental and simulated results.

$$RMSE = \sqrt{\frac{\sum_{t=1}^{n}\left(T_{B2G,t} - T_{experimental,t}\right)^2}{n}} \quad (39)$$

$$Q\ (J) = \int \dot{m}\ C_p(T_{out} - T_{in})dt \quad (40)$$

For validating the B2G coaxial model under different operating conditions, two representative days were selected: one for the summer season (cooling mode) and one for the winter season (heating mode), so the model was validated with the system injecting heat into the ground and extracting heat from the ground, respectively. Additionally, a simulation of the BHE during five days of operation was carried out in heating mode. The day selected for the summer season was the 13th of September 2018, for the winter season the 19th of November 2018 was selected and for the five days period it was selected from the 19th to 23rd of November 2018.

The soil in Tribano presented different layers of wet clay and sand, so the ground thermal properties were assumed as the average values of these materials at the different depths, in five layers. The assumed values for the ground thermal conductivity and volumetric heat capacity are presented in Table 5.

Table 5. Ground thermal properties at different depths used in the B2G model

Depth (m)	Thermal conductivity (W/(m·K))	Volumetric heat capacity (kJ/(m³·K))
0-8	1.8	2400
8-18	2.4	2500
18-21	1.8	2400
21-26	2.4	2500
26-30	1.8	2400

Considering these values presented in Table 5, the weighted average was calculated in order to determine the penetration diameters for the whole BHE depth. These average values are shown in Table 6, together with the main parameters used in the model.

Table 6. Main parameters used in the B2G coaxial model for the Tribano BHE

Thermo-physical properties		Geometrical characteristics	
Inner pipe conductivity	0.2 W/(m·K)	Length	30 m
Outer pipe conductivity	0.4 W/(m·K)	Borehole diameter	0.135 m
Average ground thermal conductivity	2.1 W/(m·K)	Inner/Outer diameter of the inner pipe	0.063/0.0514 m
Average ground volumetric thermal capacity	2450 kJ/(m³·K)	Inner/Outer diameter of the outer pipe	0.09/0.0792 m

Being no grout in the gap between the outer pipe and the borehole wall, the properties of the ground were considered in the theoretical grout region of the B2G model. The number of vertical divisions

considered in the model were 150. The simulations were carried out in a computer with a processor Intel Core i7-7700 CPU @ 3.6 GHz 3.6 GHz and 8 GB of RAM and a simulation time step of 1 minute.

As the circulation pump of the ground loop and the heat pump in the system did not stop during the night, the initial ground temperatures were not straightforward to determine. For the summer day, an undisturbed ground temperature vertical profile was used, based on the work presented in [51]; the increment of temperature due to all the heat injected and extracted during the operation of the system from the start in February was calculated using an Infinite Line Source solution approach, described in [48]. With this approach it was possible to calculate the ground temperature change at different distances from the BHE, considering all the heat injection and extraction during a determined period. So, the vertical temperature profile was determined based on the undisturbed ground profile, adding the calculated temperature increase at the different ground nodes distances (determined by the penetration diameters shown in Table 7). This solution considers the total heat transfer in the entire BHE field (calculated from the monitored data) and the interaction between the BHEs in the specified field configuration.

Regarding the initial and undisturbed ground temperatures for the winter day, an estimation was carried out based on the monitoring data measured inside the observation boreholes.

4 Results and discussion

The penetration diameters calculated inside the model, according to the correlations presented in section 2.4.2, are shown in Table 7 for the different heat injection periods: one day or five days, considering the average thermal properties of the ground.

Table 7. Penetration diameters for the Tribano BHE model at different heat injection times

Heat injection time	D_{gp1} (m)	D_{gp2} (m)	D_{ug} (m)
24 hours	0.40	0.80	1.25
120 hours	0.66	1.52	2.53

The simulations were carried out with a time step of 1 minute, the inlet temperature measured at the head of the BHE8 was introduced as an input in the model and a constant flow rate of 400 kg/h was assumed. The simulated outlet temperature was compared with the measured outlet temperature at the head of the BHE8. The results of the different simulations are shown in Figure 8 for the summer day, in Figure 9 for the winter day and in Figure 10 for the simulation of the operation during five days. The simulation time for the daily simulations was around 2.5 seconds, while the simulation time of the five days operation was around 7.2 seconds.

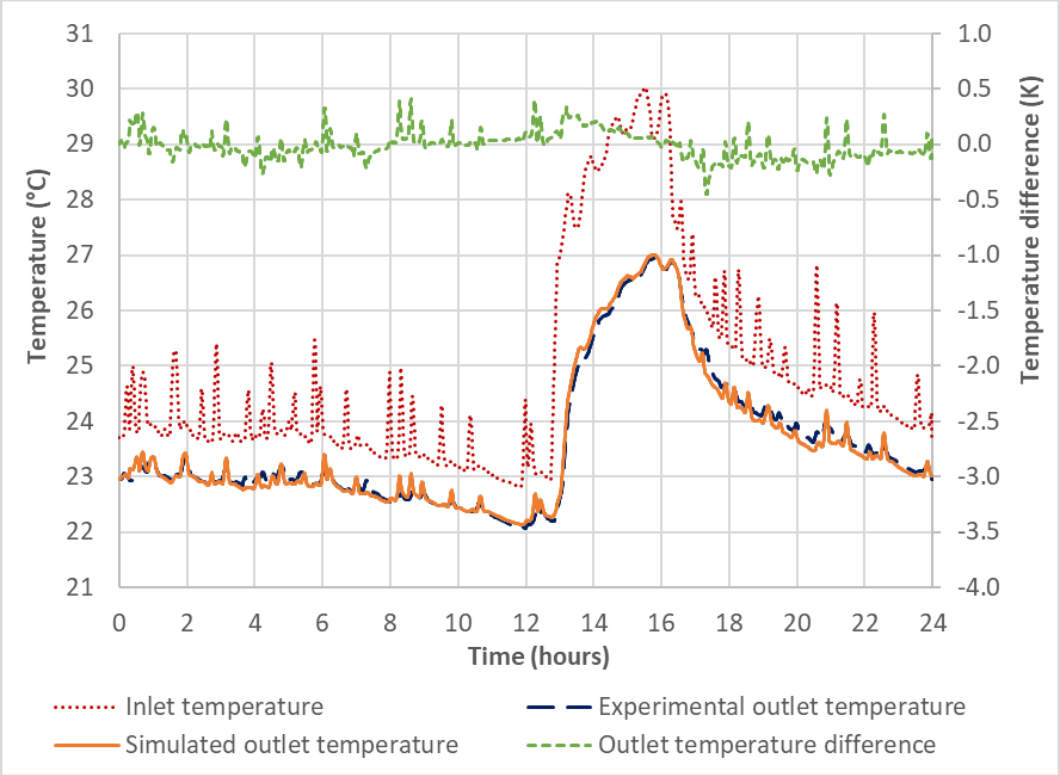

Figure 8. B2G coaxial summer day operation (13/09/2018): simulation results

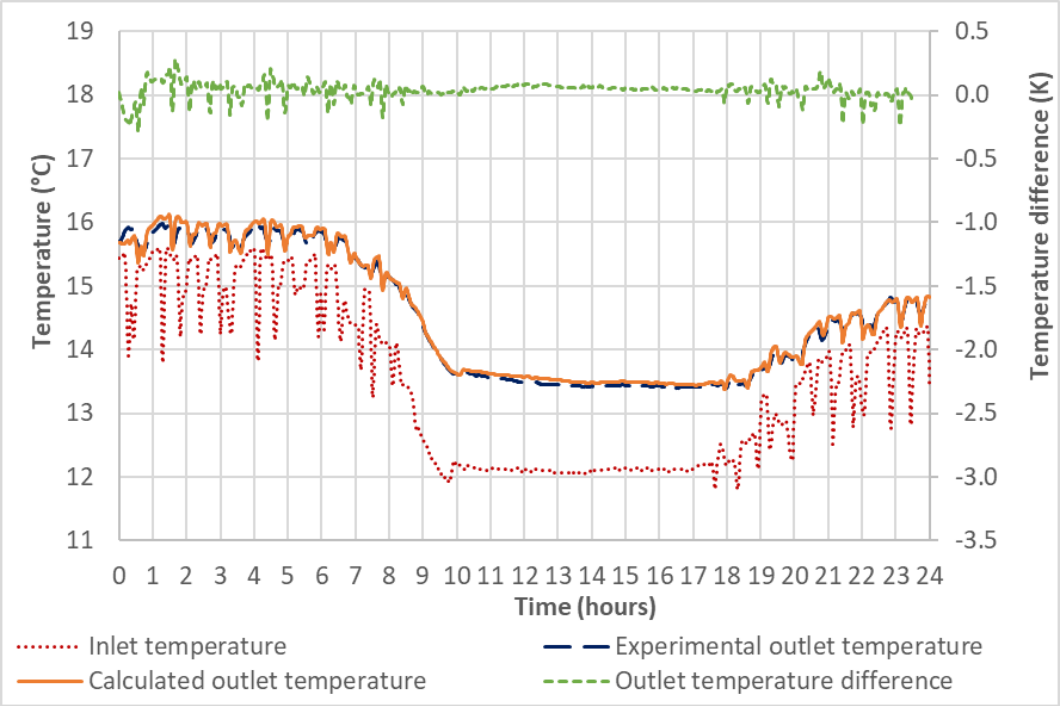

Figure 9. B2G coaxial winter day operation (19/11/2018): simulation results

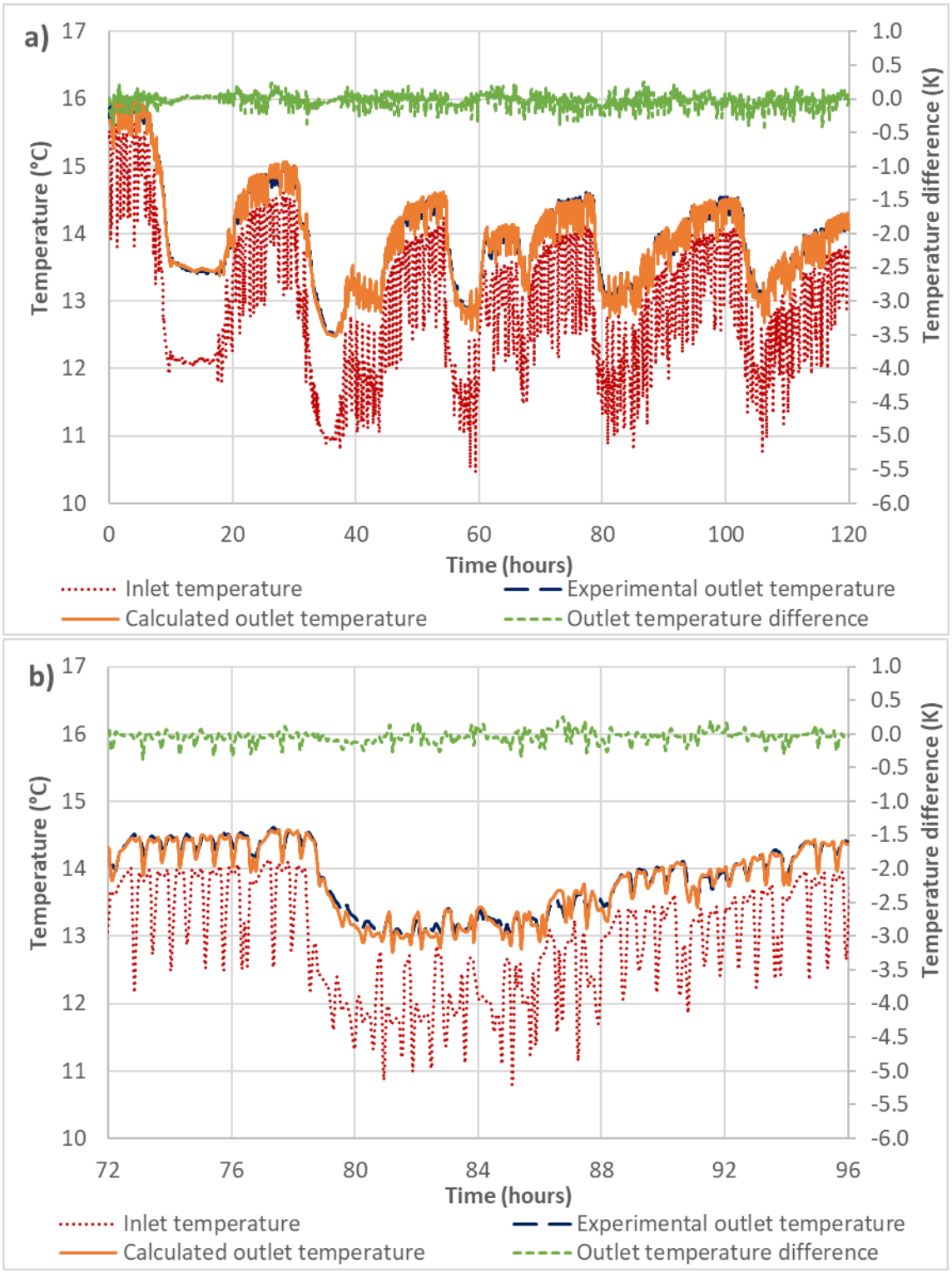

Figure 10. B2G coaxial five winter days operation (19/11/2018-23/11/2018): a) simulation results for the five days; b) zoom on the fourth day.

The simulated results have confirmed a good agreement with the experimental measurements in all the cases. The RMSE, the highest temperature error and the difference in the heat transfer between the simulated and experimental results are shown in Table 8. The RMSE are lower than 0.1 K in the winter days simulation, while it is around 0.12 K for the summer day simulation. The difference in the heat transfer is lower than 4% in all the cases.

Table 8. B2G coaxial daily operation in Tribano: calculated errors

	RMSE (K)	Highest outlet temperature difference (K)	Calculated heat transfer from data (kJ)	Simulated heat transfer (% of experimental)
Summer day	0.1209	0.4530	51140	+0.91%
Winter day	0.0747	0.2857	41716	+3.43%
5 winter days	0.0875	0.4177	198087	-2.06%

5 Conclusions

A new dynamic model, able to accurately reproduce the short-mid term (up to five days) behaviour of a coaxial BHE with a low computational time was developed (B2G model) and implemented in TRNSYS.

The B2G model was previously developed for a U-tube BHE configuration by the same research group and now it has been adapted to a coaxial configuration and upgraded with several new features (vertical heat conduction, heterogeneous ground and higher number of ground nodes). Furthermore, polynomial correlations were obtained to calculate the optimal position of the ground nodes and were implemented inside the B2G model to automatically calculate this position depending on the thermo-physical properties of the ground, the BHE geometry and the operating conditions of the system (heat injection period during a day). As a result, the B2G model can be used as a black box in an integrated GSHP system model in TRNSYS to predict the short-mid term behaviour of the ground loop and provide an accurate inlet to the heat pump in order to simulate its performance and the coupling with the rest of the system.

The model validation with the dual source heat pump installation of Hiref headquarters in Tribano (Italy) presented a good agreement (RMSE<0.12 K) between the simulated results and the experimental data, confirming that the B2G model correctly reproduces the short-mid term response of the coaxial BHE.

Abbreviations

α	thermal diffusivity (m^2/s)
A	area (m^2)
B2G	Borehole-To-Ground (BHE dynamic model)
BHE	Borehole Heat Exchanger
c	volumetric thermal capacity ($J/m^3 \cdot K$)
C	thermal capacitance (J/K)
C_p	heat capacity ($J/kg \cdot K$)
D	diameter (m)
DSHP	Dual Source Heat Pump
Fo	Fourier number (-)
GSHE	Ground Source Heat Exchanger
GSHP	Ground Source Heat Pump
h	convective heat transfer coefficient ($W/m^2 \cdot K$)
k	conductivity ($W/m \cdot K$)
λ	thermal conductivity ($W/(m \cdot K)$)
$\dot{m}$	mass flow rate (kg/s)
n	number of nodes (-)
OB	Observation Borehole
q	heat flux (W/m)
r	radial distance (m)
R	thermal resistance (K/W) / penetration radius (m)
RMSE	Root Mean Square Error
ρ	density (kg/m^3)
t	time (s)
T	temperature (C)
U	overall heat transfer coefficient ($W/(m^2 \cdot K)$)
v	velocity (m/s)
z	borehole depth coordinate (m)

Subscripts

0	initial point
b	borehole / grout
bg1	borehole node to short term ground node
ci	inner diameter of the inner pipe
co	outer diameter of the inner pipe
ei	inner diameter of the outer pipe
eo	outer diameter of the outer pipe
g	ground
g1	ground node (short term)
g2	ground node (mid-term)
g1g2	short term to mid-term ground nodes
gp1	ground penetration for short term ground node
gp2	ground penetration for mid-term ground node
h	convection
i	inner pipe zone
ip	inner pipe
in	inlet
io	inner pipe node to outer pipe node
j	j-node
o	outer pipe zone
op	outer pipe
out	outlet
ob	outer pipe zone to borehole backfilling node
ug	undisturbed ground
x	borehole node position

Acknowledgements

The present work has been supported by the European Community Horizon 2020 Program for European Research and Technological Development (2014-2020) inside the framework of the project 656889 – GEOTeCH (Geothermal Technology for Economic Cooling and Heating) and by the

Generalitat Valenciana inside the program “Ayudas para la contratación de personal investigador en formación de carácter predoctoral (ACIF/2016/131)”.

The authors would like to acknowledge Eng. PhD. Giulio Busato and Eng. Alessandro Zerbetto, from the company HiRef S.p.A. for providing the information about the installation and its operation, and Dr. Henk Witte, from Groenholland B.V. for the monitored data. Also the team from the University of Padua (Dr. Marco Azzolin, Dr. Stefano Bortolin, Eng. Emanuele Zanetti and Prof. Davide del Col), for helping in the analyisis of the data.

Special thanks to the Georesources team of University of Bologna (Dr. Sara Kasmaee, Dr. Sara Focaccia, Eng. Kristina Strpić and Dr. Carlo Cormìo) for all their support during the calibration activities of ground and circuit temperature measurements and interpretation of geological data.

References

[1] International Energy Agency. Energy Efficiency 2017. IEA; 2017.

[2] Rees SJ. Advances in Ground-Source Heat Pump Systems. Woodhead Publishing; 2016.

[3] Carvalho AD, Moura P, Vaz GC, De Almeida AT. Ground source heat pumps as high efficient solutions for building space conditioning and for integration in smart grids. Energy Convers Manag 2015;103:991–1007. doi:10.1016/j.enconman.2015.07.032.

[4] Urchueguía JF, Zacarés M, Corberán JM, Montero Á, Martos J, Witte H. Comparison between the energy performance of a ground coupled water to water heat pump system and an air to water heat pump system for heating and cooling in typical conditions of the European Mediterranean coast. Energy Convers Manag 2008;49:2917–23. doi:10.1016/j.enconman.2008.03.001.

[5] Florides G, Kalogirou S. Ground heat exchangers—A review of systems, models and applications. Renew Energy 2007;32:2461–78. doi:10.1016/j.renene.2006.12.014.

[6] Gordon D, Bolisetti T, Ting DSK, Reitsma S. A physical and semi-analytical comparison between coaxial BHE designs considering various piping materials. Energy 2017;141:1610–21. doi:10.1016/j.energy.2017.11.001.

[7] Kurevija T, Macenić M, Strpić K. Steady-State Heat Rejection Rates for a Coaxial Borehole Heat Exchanger During Passive and Active Cooling Determined With the Novel Step Thermal Response Test Method. Rud Zb 2018;33:61–71. doi:10.17794/rgn.2018.2.6.

[8] Acuña J. Distributed thermal response tests – New insights on U-pipe and Coaxial heat exchangers in groundwater-filled boreholes. KTH, 2013.

[9] Focaccia S, Tinti F. An innovative Borehole Heat Exchanger configuration with improved heat transfer. Geothermics 2013;48:93–100. doi:10.1016/J.GEOTHERMICS.2013.06.003.

[10] Carslaw HS, Jaeger JC. Conduction of heat in solids. Second ed. New York, NY, USA: Oxford University Press; 1959.

[11] Al-Khoury R. Computational Modeling of Shallow Geothermal Systems. CRC Press; 2012.

[12] Yang H, Cui P, Fang Z. Vertical-borehole ground-coupled heat pumps: A review of models and systems. Appl Energy 2010;87:16–27. doi:10.1016/j.apenergy.2009.04.038.

[13] Eskilson P, Claesson J. Simulation model for thermally interacting heat extraction boreholes. Numer Heat Transf 1988;13:149–65. doi:10.1080/10407788808913609.

[14] Yang W, Shi M, Liu G, Chen Z. A two-region simulation model of vertical U-tube ground heat exchanger and its experimental verification. Appl Energy 2009;86:2005–12. doi:10.1016/j.apenergy.2008.11.008.

[15] Bauer D, Heidemann W, Müller-Steinhagen H, Diersch H-JG. Thermal resistance and capacity models for borehole heat exchangers. Int J Energy Res 2011;35:312–20. doi:10.1002/er.1689.

[16] Pasquier P, Marcotte D. Short-term simulation of ground heat exchanger with an improved TRCM. Renew Energy 2012;46:92–9. doi:10.1016/j.renene.2012.03.014.

[17] Lamarche L, Kajl S, Beauchamp B. A review of methods to evaluate borehole thermal resistances in geothermal heat-pump systems. Geothermics 2010;39:187–200. doi:10.1016/j.geothermics.2010.03.003.

[18] Zarrella A, Scarpa M, De Carli M. Short time step analysis of vertical ground-coupled heat exchangers: The approach of CaRM. Renew Energy 2011;36:2357–67. doi:10.1016/J.RENENE.2011.01.032.

[19] Li M, Lai ACK. New temperature response functions (G functions) for pile and borehole ground heat exchangers based on composite-medium line-source theory. Energy 2012;38:255–63. doi:10.1016/J.ENERGY.2011.12.004.

[20] Javed S, Claesson PEJ. New analytical and numerical solutions for the short-term analysis of vertical ground heat exchangers. ASHRAE Trans 2011;117:3–12.

[21] Spitler JD. GLHEPRO – A DESIGN TOOL FOR COMMERCIAL BUILDING GROUND LOOP HEAT EXCHANGERS. Proc. Fourth Int. Heat Pumps Cold Clim. Conf., Aylmer, Québec: 2000, p. 17–8.

[22] Blomberg T, Claesson J, Eskilson P, Hellström G, Sanner B. EED - Earth Energy Designer 2016.

[23] Department Of Energy. EnergyPlus 1998.

[24] Klein SA, Beckman WA, Duffie JA. TRNSYS: A Transient System Simulation Program 2007.

[25] Klein SA, Beckman WA, Duffie JA. TRNSYS - a transient simulation program. ASHRAE Trans. 82, Dallas: 1976.

[26] Eskilson P. Superposition borehole model. Manual for computer code. Lund, Sweden: Department of Mathematical Physics, Lund Institute of Technology; 1986.

[27] Eskilson P. Thermal Analysis of Heat Extraction Boreholes. University of Lund, 1987.

[28] Pahud D, Fromentin A, Hadorn J-C. The Superposition Borehole Model for TRNSYS (TRNSBM) 1996.

[29] Pahud D. The Superposition Borehole Model for TRNSYS 16 or 17 (TRNSBM) 2012:1–16.

[30] Hellström G. Duct ground heat storage model. Manual for computer code 1989.

[31] Hellström G. Ground Heat Storage. Thermal Analyses of Duct Storage Systems. University of Lund, 1991.

[32] Pahud D, Hellström G. The new duct ground heat model for TRNSYS. In: Van Steenhoven AA, Van Helden WGJ, editors. Eurotherm Semin. nº49, Phys. Model. Therm. Energy Stores, Eindhoven, The Netherlands: 1996, p. 127–36.

[33] Pahud D, Hellström G, Mazzarella L. Duct ground heat storage model for TRNSYS (TRNVDST). User manual 1997.

[34] Pärisch P, Mercker O, Oberdorfer P, Bertram E, Tepe R, Rockendorf G. Short-term experiments with borehole heat exchangers and model validation in TRNSYS. Renew Energy 2015;74:471–7. doi:10.1016/j.renene.2014.07.052.

[35] Ruiz-Calvo F, De Rosa M, Acuña J, Corberán JM, Montagud C. Experimental validation of a short-term Borehole-to-Ground (B2G) dynamic model. Appl Energy 2015;140:210–23. doi:10.1016/j.apenergy.2014.12.002.

[36] De Rosa M, Ruiz-Calvo F, Corberán JM, Montagud C, Tagliafico LA. A novel TRNSYS type for short-term borehole heat exchanger simulation: B2G model. Energy Convers Manag 2015;100:347–57. doi:10.1016/j.enconman.2015.05.021.

[37] Ruiz-Calvo F, De Rosa M, Monzó P, Montagud C, Corberán JM. Coupling short-term (B2G model) and long-term (g-function) models for ground source heat exchanger simulation in TRNSYS. Application in a real installation. Appl Therm Eng 2016;102:720–32. doi:10.1016/j.applthermaleng.2016.03.127.

[38] Cazorla-Marin A, Montagud C, Corberán JM, Acuña J. Modeling of a coaxial Borehole Heat Exchanger and experimental validation. 10º Congr. Int. Ing. Termodinámica 10CNIT, LLeida, Spain: 2017, p. 162–3.

[39] Cazorla-Marin A, Montagud C, Corberán JM. Adaptation of the B2G dynamic model to new borehole heat exchanger coaxial configurations. IX Congr. Ibérico y VII Congr. Iberoam. Ciencias y Técnicas del Frío - CYTEF2018, Valencia, Spain: Instituto de Ingeniería Energética. Universitat Politècnica de València; 2018, p. 1186.

[40] Cazorla-marín A, Ruiz-calvo F, Witte H, Montagud C, Corberán JM. An Innovative Co-Axial Spiral Borehole Heat Exchanger Dynamic Model. Eur. Geotherm. Congr. 2016, Strasbourg, France: EGEC; 2016, p. T-UTES-127.

[41] Cazorla-Marin A, Montagud C, Witte H, Hylkema R, Corberan J. Modelling and Experimental Validation of a Novel Co-axial Spiral Borehole Heat Exchanger. In: Spitler JD, Bernier M, Fang Z, Gehlin S, Rees SJ, editors. IGSHPA Res. Conf. Proc., Denver, USA: International Ground Source Heat Pump Association; 2017, p. 212–20. doi:10.22488/okstate.17.000503.

[42] Melinder Å. Properties of Secondary Working Fluids for Indirect Systems. Paris, France: International Institute of Refrigeration, IIR; 2010.

[43] Gnielinski V. G1 Heat Transfer in Pipe flow. In: VDI-Gesellschaft Verfahrenstechnik und Chemieingenieurwesen, editor. VDI Heat Atlas. Second Edi, Düsseldorf: Springer-Verlag Berlin Heidelberg; 2010.

[44] Lax P, Wendroff B. Systems of conservation laws. Commun Pure Appl Math 1960;13:217–37. doi:10.1002/cpa.3160130205.

[45] Hart DP, Couvillion R. Earth-Coupled Heat Transfer. Dubil, OH: National Water Well Association; 1986.

[46] Cazorla-Marín A, Montagud C, Corberán JM, Tinti F, Focaccia S. Upgrade of the B2G dynamic geothermal heat exchanger model: optimal location of the ground nodes. In: Spitler J, Acuña J, Bernier M, Fang Z, Gehlin S, Javed S, et al., editors. IGSHPA Res. Track 2018, Stockholm, Sweden: International Ground Source Heat Pump Association; 2018, p. 20–8. doi:10.22488/okstate.18.000013.

[47] MathWorks. Global Optimization Toolbox - User's Guide - MATLAB. 2017.

[48] Cazorla-Marín A. Modelling and experimental validation of an innovative coaxial helical borehole heat exchanger for a dual source heat pump system. Universitat Politècnica de València, 2019.

[49] European Commission. Geothermal Technology for €conomic Cooling and Heating (H2020-LCE-2014-2, GEOTeCH-656889) 2015. http://www.geotech-project.eu/ (accessed January 20, 2019).

[50] HiRef S.p.A. HiRef n.d. https://hiref.it/en (accessed January 25, 2019).

[51] Tinti F, Carri A, Kasmaee S, Valletta A, Segalini A, Bonduà S, et al. Ground temperature monitoring for a coaxial geothermal heat exchangers field: practical aspects and main issues

from the first year of measurements. Mining-Geology-Petroleum Eng Bull 2018;33:47–57. doi:10.17794/rgn.2018.5.5.

[52] Groenholland BV. Groenholland Geo Energy Systems n.d. http://www.groenholland.com/en/ (accessed March 13, 2019).

Declaration of interests: none